

PAPERS

Metal wire network based transparent conducting electrodes fabricated using interconnected crackled layer as template

To cite this article: S Kiruthika *et al* 2014 *Mater. Res. Express* 1 026301

View the [article online](#) for updates and enhancements.

Related content

- [A cracked polymer templated Ag network for flexible transparent electrodes and heaters](#)
Chaoting Zhu, Ruiqin Tan, Weijie Song *et al.*
- [Enhancement of electrical conductivity of silver nanowires-networked films via the addition of Cs-added TiO₂](#)
Sunho Kim, Haksoo Lee, Sekwon Na *et al.*
- [Silver nanowire-graphene hybrid transparent conductive electrodes for highly efficient inverted organic solar cells](#)
Neng Ye, Jieli Yan, Shuang Xie *et al.*

Recent citations

- [Narrowing desiccating crack patterns by an azeotropic solvent for the fabrication of nano-mesh electrodes](#)
Rajashekhar Pujar *et al*
- [Flexible, quickly responsive and highly efficient E-heating carbon nanotube film](#)
Mohamed Amine Aouraghe *et al*
- [A spring network simulation in three dimensions for designing optimal crack pattern template to fabricate transparent conducting electrodes](#)
Supti Sadhukhan *et al*



IOP | ebooks™

Bringing you innovative digital publishing with leading voices to create your essential collection of books in STEM research.

Start exploring the collection - download the first chapter of every title for free.

Metal wire network based transparent conducting electrodes fabricated using interconnected crackled layer as template

S Kiruthika¹, K D M Rao¹, Ankush Kumar, Ritu Gupta and G U Kulkarni

Chemistry & Physics of Materials Unit and Thematic Unit of Excellence in Nanochemistry, Jawaharlal Nehru Centre for Advanced Scientific Research, Jakkur P.O., Bangalore-560 064, India

E-mail: kulkarni@jncasr.ac.in

Received 13 November 2013, revised 17 February 2014

Accepted for publication 11 March 2014


Published 3 April 2014

Materials Research Express 1 (2014) 026301

doi:[10.1088/2053-1591/1/2/026301](https://doi.org/10.1088/2053-1591/1/2/026301)

Abstract

A metal (Au) wire network, nearly invisible to the naked eye, has been realized on common substrates such as glass, to serve as a transparent conducting electrode (TCE). The process involves coating a TiO₂ nanoparticle dispersion to a film thickness of $\sim 10\ \mu\text{m}$, which following solvent evaporation, spontaneously forms a crackle network; the film is then used as a sacrificial template for metal deposition. The TCE thus formed exhibited visible transmittance of $\sim 82\%$ and sheet resistance of $3\text{--}6\ \Omega/\text{square}$ for a metal fill factor of 7.5% . With polyethylene terephthalate substrate, flexible and robust TCE could be produced and with quartz, the spectral range could be widened to cover UV and IR regions.

 Online supplementary data available from stacks.iop.org/MRX/1/026301/mmedia

Keywords: colloidal TiO₂, crackle layer, metal network, transparent conductor, flexible electronics

1. Introduction

Particulate films exhibit cracks above a critical thickness, due to the stress induced by solvent evaporation [1], which is widely seen in nature such as in mud cracking [2–4]. Cracks, by definition, are unpredictable and widely varied [5, 6]. Indeed, a crack is something one wishes to avoid at any cost. In thin film based device fabrication, the occurrence of cracking is

¹ These authors have contributed equally.

considered detrimental to the device performance and its reproducibility [7]. There have been efforts in the literature to inhibit crack formation by manipulating the stress [6–8]. Thus, Prosser *et al* [8] followed an unconventional deposition process, in which a thick film of ~ 500 nm was obtained by sequential deposition of thin layers, each below the critical thickness. In another instance [9], the crack formation in a TiO_2 nanoparticle layer used in solar cell fabrication, was suppressed by applying pressure during drying. In contrast to the above reports, there are recent indications in the literature of exploiting cracks for material deposition and patterning [10]. In an interesting report using cracks formed in a TiO_2 nanoparticle layer coated on graphene, the latter was given mild exposure to acid vapor through cracks so as to control its doping [11]. This is an example of using a cracked layer as a lithography template. Recently, Wei Han *et al* [12] have reported crack formation in films of polystyrene beads which formed a template for Au wire. Here, we report a method to fabricate a highly extended metal wire network employing cracked TiO_2 layer as a template. A transparent substrate supporting the metal nanowire network essentially constitutes a transparent conducting electrode.

There is much emphasis in the literature given to the fabrication of transparent conducting electrodes using nanomaterials such as CNTs [13–15], metal nanowires [16–20] and graphene [21–27] as possible replacements for the conventional electrode material, tin doped indium oxide (ITO), as the processing costs are high and In is relatively less abundant [28, 29]. ITO possesses properties rightly suited to optoelectronic applications; typically, ITO films exhibit transmittance of 92% for visible wavelengths and sheet resistance, $10 \Omega/\text{square}$, which explains the widespread use [30–32]. The new generation alternative electrodes, which essentially consist of percolative conducting networks of 1D nanomaterials (CNTs or Ag nanowires) deposited on common substrates such as glass or PET wherein the nude areas amidst the network transmit light [33]. In such a situation, as is obvious, there is always a trade-off between the transmittance and the sheet resistance, which is achieved by optimising the nanomaterial loading. Thus, performance specifications close to if not better than ITO, have been reported [34, 35]. The challenge is, of course, the optimisation step of ensuring uniform loading of the conducting network over macro-areas while minimising the contact resistance and occurrence of redundant wires (or tubes), which remain unconnected to rest of the network [36, 37]. Secondly, the roughness associated with the network can be a nightmare in thin film device fabrication involving macro-areas [38, 39]; a few nanowires or tubes which, during deposition and subsequent processing, happen to raise themselves from the average network thickness, can actually shunt the device [40–44]. Prompted by the above observations, we considered it interesting to explore the possibility of forming a wire network by metal vapor deposition, using a cracked layer of TiO_2 nanoparticles as a sacrificial template.

2. Experimental

2.1. Fabrication of transparent conducting electrode

TiO_2 nanoparticle powder (80 mg, P25 Degussa) was dispersed in 1 mL of ethanol by rigorously ultrasonication for 1 h to form a suspension. Further, 0.16 mL of ethyl acetate was added to the suspension to enhance the crackle formation with lesser film thickness. It was then used directly for drop coating on various substrates (glass, quartz and PET). The volume of solution varied with respect to the substrate size. Typically, $30 \mu\text{L}$ was drop-coated per cm square area of the substrate. The crackle network pattern formed spontaneously in the coated

layer was left to dry in air. Au metal was deposited by physical vapor deposition system (Hind High Vacuum Co., India). The TiO₂ template was lifted-off from the substrate by washing in water with mild sonication.

2.2. Characterization

Transmittance was measured over a range of 200–3000 nm using a UV/visible/near-IR spectrophotometer from Perkin-Elmer (Lambda 900). Sheet resistance was measured using a 4-pin setup (Techno Science Instruments, India). Low temperature measurements were done using a THMS600 stage from Linkam Scientific Instruments Ltd, UK. SEM was carried out using a Nova NanoSEM 600 instrument (FEI Co., The Netherlands). Energy-dispersive spectroscopy (EDS) analysis was performed with an EDAX Genesis instrument (Mahwah, NJ) attached to the SEM column. AFM measurements were performed using di Innova (Bruker, USA) in contact mode. Standard Si cantilevers were used for normal topography imaging. Wyko NT9100 optical profiling system (Bruker, USA) was used for height and depth measurements. ImageJ software was used to perform analysis of the crackle patterns. The change in resistance during bending, flexibility and adhesion test was measured using a multimeter interfaced with computer using DMM viewer software. For thermal imaging, the electrode contacts were established using thick epoxy Ag paint. The substrate was mounted with supports at both ends such that it is kept hanging in air while the imaging is done from the front view of the electrode. The voltage was applied using Keithley 2400 and thermal imaging was carried out using Testo thermal imager (Testo 885). The thermal images were analysed using the offline software.

3. Results and discussion

The process consists of only three steps (schematic in figure 1(a)). A smooth transparent substrate (glass, quartz or PET) is drop coated with a colloidal dispersion of TiO₂ nanoparticles (~ 21 nm) in ethanol-ethyl acetate mixture (0.08 g mL^{-1}) to a thickness of $\sim 13 \mu\text{m}$ which was allowed to dry under ambient conditions. The dispersion was chosen after several optimisation trials (figure S1 in the supplementary data). As shown in figure 1(b), the TiO₂ layer formed cracks all over the substrate with two remarkable features—all cracks were interconnected to give rise to a single network and the cracking was complete with no residual layer at the bottom, as revealed by the light tracks seen in the transmission mode microscopy (figures 1(b) and S2 in the supplementary data). More appropriately, these are crackles. Importantly as shown in the SEM image in figure 1(c), the crack width is in the range $3\text{--}20 \mu\text{m}$ and the crack spacing, $50\text{--}200 \mu\text{m}$, which makes the study worthwhile. The TiO₂ nanoparticles are seen densely stacked in the dried film (figure 1(d)) giving way to clean cracked regions—lines, curves and junctions alike. In the second step, Au was deposited by vacuum evaporation to a thickness of ~ 100 nm. Following developing in water (third step), the TiO₂ nanoparticles could be lifted-off the substrate leaving behind the metal trapped inside the cracked regions (see schematic in figure 1(a)). The AFM topography images and the z-profiles derived from them (figures 1(e) and S3 in the supplementary data) showed that the widths associated with the crack and the metal retained on the substrate after lift-off are similar. The Au wire network thus formed was examined using SEM and Au M signal in energy-dispersive spectroscopy (EDS). As shown in the images in figures 1(f) and (g), the material retained on the substrate was indeed the Au wire network (see EDS spectrum in figure 1(g)). The wire roughness measured over 1.3 mm^2 using

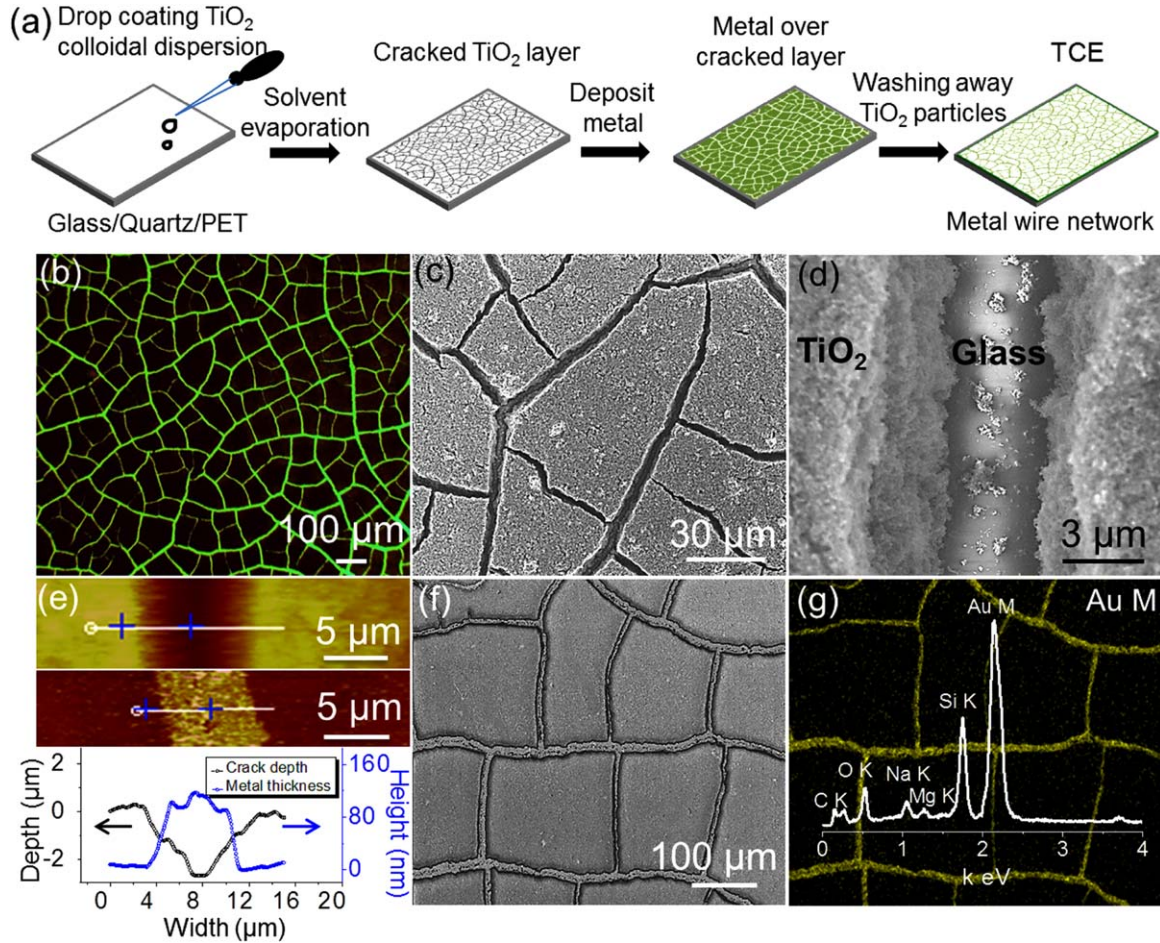


Figure 1. (a) Schematic of the TCE fabrication. Below (b) optical microscopy image showing a network of cracks in a dried TiO₂ nanoparticle layer on glass. The image was recorded in the transmission mode with a green light source illuminating from below. (c) SEM image of the cracked layer. (d) A magnified image showing densely packed TiO₂ nanoparticles on the wall of the crackle. (e) AFM topography images of a crack (top) and metal wire (middle) and the corresponding z-profiles (bottom). (f) SEM image of the Au wire network and (g) Au M EDS map and the total spectrum. Other peaks are due to the glass substrate.

optical profilometry is shown in the supplementary data (figure S3). The arithmetic mean value (R_a) was 2.63 nm from the wire network surface, while the maximum roughness height (R_t) was 102 nm due to the thickness of nanowire.

The Au wire network based TCEs supported on glass, quartz and PET, exhibited transmittance of ~82% (figure 2(a)), not only in the visibly relevant region (see photographs) but also beyond, up to 1500 nm for PET and glass, and 3000 nm for quartz. This was possible because the metal fill factor was only ~7.5% (figure S4). Quartz allowed UV light down to 200 nm (figure S5 in the supplementary data), qualifying as a TCE with wide spectral range. The sheet resistance values measured using a four-pin setup was in the range of 3–6 Ω/square for the different TCEs. These values are comparable to, or in many instances, even better than those of ITO films and other nanowire or nanotube based TCEs. What may further attract one's

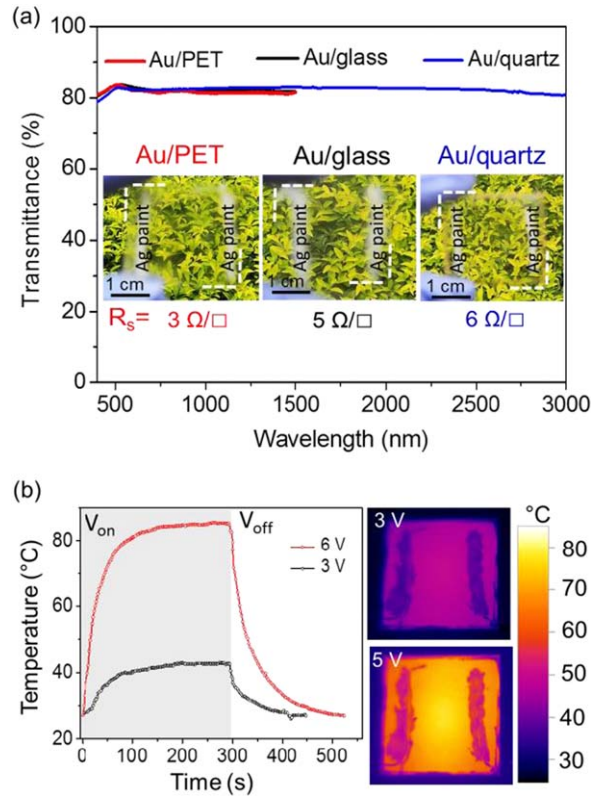


Figure 2. (a) A plot of transmittance versus wavelength of light obtained for Au wire networks on glass (black), quartz (blue) and PET (red). Photographs of the substrates held using fingers against a plant are shown along with four probe sheet resistance values. (b) Variation in the temperature as measured using an IR camera, of Au/quartz based TCE with time, after applying different voltages across silver contact pads. The corresponding thermographs depicting temperature variations after reaching saturation are shown on the right.

attention are the simplicity of process steps, inexpensive tools and environmentally friendly raw materials.

In order to reveal the overall presence of the Au wire network, we applied a small bias across two Ag epoxy contacts and joule heated the TCE. As shown in figure 2(b), the temperature of the Au/quartz TCE rose, in a matter of seconds, to a value which increased with increasing bias voltage. This is, in principle, a transparent heater. The thermographs shown on the right in figure 2(b), confirm the presence of the resistive wire network across the substrate. The uniform temperature distribution indicates good electrical connectivity of the network throughout the substrate, devoid of junction contact resistance.

For efficient active layer-electrode interface in optoelectronic devices, it is required to produce smaller metal wire widths which in turn demands, in this study, fine crackles in the nanoparticle film. Crack spacing and width can be reduced by decreasing the thickness of the film, but this is limited by the critical film thickness, below which less interconnected cracks are observed (figure S1 in the supplementary data). We have explored the possibility of reducing crackle width by reducing the film drying temperature, thereby slowing down solvent evaporation. Crackle networks in TiO_2 nanoparticle films (all $\sim 30 \mu\text{m}$ thick) dried at various

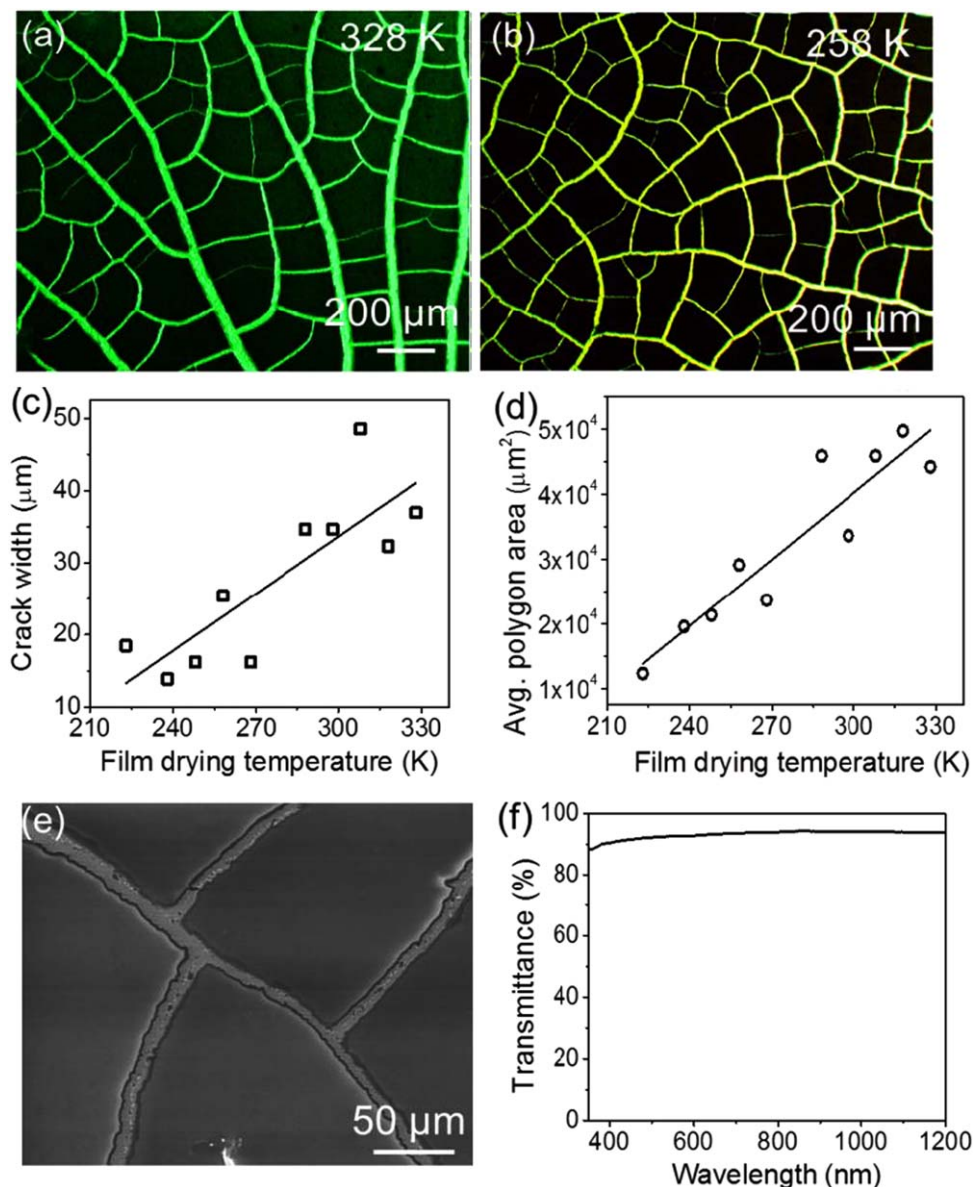


Figure 3. Optical microscopic images of interconnected crackles formed in TiO₂ nanoparticle film when dried at 328 K (a) and 258 K (b) under nitrogen flow. (c) A plot of maximum crack width versus the drying temperature. (d) A plot of average polygon area of crackles versus the drying temperature. (e) SEM image of Au networked wire on glass obtained using the 258 K dried film. (f) Transmittance spectrum of the Au/glass TCE.

temperatures are shown in figure S6 in the supplementary data. As is evident, the crackle widths as well as the polygon areas are found to decrease at lower drying temperature (compare figures 3(a) and (b)) due to slower evaporation of the solvents, which obviously influences the stress release in the film. At low drying temperatures, the network often contained fine crackles of width $<1\ \mu\text{m}$ (figure S7 in the supplementary data). The maximum crackle width decreased from $37\ \mu\text{m}$ at 328 K to $18\ \mu\text{m}$ at 223 K and the variation was nearly linear with some spread

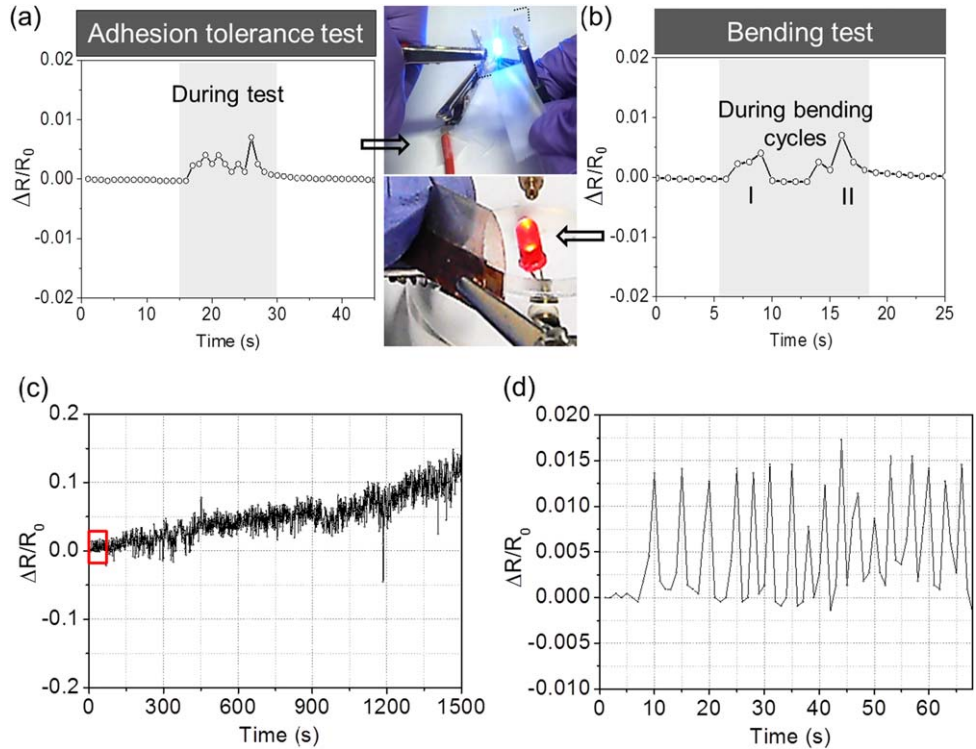


Figure 4. (a) A Au/PET substrate subjected to scotch tape adhesion test. The Au wire network was connected in series to an LED circuit. The relative change in resistance during the test is shown left. (b) The relative change in resistance during the bending cycles. The glowing LED is shown on the left. (c) The resistance of the TCE during several cycles of bending. The portion marked in the red box is shown magnified in (d). The resistance variation during each cycle is less than 2%.

(figure 3(c)). Concomitantly, the average area per polygon, calculated by dividing the total area ($\sim 2.4 \text{ mm}^2$) with the number of polygons, was also found to vary linearly (figure 3(d)). Below 223 K, drying the nanoparticle film proved practically difficult. A Au wire TCE (figure 3(e)) fabricated using a 258 K dried film exhibited transmittance of $\sim 93\%$ (figure 3(f)), much higher than the metal network formed from the room temperature crackle network ($\sim 82\%$, figure 2(a)). The sheet resistance of TCE fabricated from film dried at 258 K was $32.5 \Omega/\text{square}$. However, this process needed further optimisation for producing large area TCEs. Another important parameter which can be explored to tune crack spacing and width, is the particle size [1, 45, 46]. TiO_2 nanoparticles having diameter of $\sim 16 \text{ nm}$ were prepared [47] which produced cracks with much finer widths (see figure S8 in the supplementary data).

PET is commonly used as a substrate for flexible optoelectronics. In this context, we have examined the robustness of the Au/PET based TCE by taking it through adhesion and flexibility tests (figure 4). Sticking a scotch tape, pressing and peeling off from the TCE surface caused less than 1% change in the resistance, that being temporary (figures 4(a) and S9(a) in the supplementary data and Movie in the supplementary data). Upon bending over several cycles (figures 4(b)–(d)), we observed similar mild changes in the TCE resistance. Such was the case during crumbling, rolling and twisting (figure S9(b) in the supplementary data). The PET substrate hosting the delicate Au wire network could withstand all aggressive handling.

4. Conclusions

We have developed a simple method for the fabrication of transparent conducting electrodes consisting of a Au micro/nanowire network on a transparent substrate produced using a crackled TiO₂ nanoparticle film as a template. This is a spontaneously formed template unlike those used in conventional lithography techniques. The fabricated TCEs are commendable—they are inexpensive and robust, yet can perform with the desired optoelectronic properties required in industry. The fabrication process involves materials that are environmentally benign. A typical TCE produced by this method exhibited transmittance ~82% in the visible range with sheet resistance of 3–6 Ω /square. Depending on the substrate property, the property of the TCE could be tuned. By using quartz as substrate, appreciable transmittance was achieved in the UV and IR ranges. Similarly, a flexible TCE was obtained using PET as the host supporting Au wire network. The method opens up a wide range of possibilities for future studies, such as the choice of metal (or material), the deposition process—physical or chemical, controlling the nanostructure etc.

Acknowledgements

The authors are grateful to Professor C N R Rao for his encouragement. The financial support from the Department of Science and Technology, Government of India, is gratefully acknowledged. SK and KDMR acknowledge DST-INSPIRE and UGC for fellowships, respectively. The authors thank N R Selvi for SEM and EDS imaging and Dr S Basavaraj for his assistance in AFM.

Patent information: Indian Patent Application No. 954/CHE/2013 filed on 5 March 2013.

References

- [1] Lee W P and Routh A F 2004 Why do drying films crack? *Langmuir* **20** 9885–8
- [2] Pasricha K, Wad U, Pasricha R and Ogale S 2009 Parametric dependence studies on cracking of clay *Physica A* **388** 1352–8
- [3] Goehring L, Conroy R, Akhter A, Clegg W J and Routh A F 2010 Evolution of mud-crack patterns during repeated drying cycles *Soft Matter* **6** 3562–7
- [4] Groisman A and Kaplan E 1994 An experimental study of cracking induced by desiccation *EPL* **25** 415
- [5] Alava M J, Nukala P K and Zapperi S 2006 Statistical models of fracture *Adv. Phys.* **55** 349–476
- [6] Ngo A T, Richardi J and Pileni M P 2013 Crack patterns in superlattices made of maghemite nanocrystals *Phys. Chem. Chem. Phys.* **15** 10666–72
- [7] Park J T, Chi W S, Roh D K, Ahn S H and Kim J H 2013 Hybrid templated synthesis of crack free, organized mesoporous TiO₂ electrodes for high efficiency solid state dye sensitized solar cells *Adv. Funct. Mater.* **23** 26–33
- [8] Prosser J H, Brugarolas T, Lee S, Nolte A J and Lee D 2012 Avoiding cracks in nanoparticle films *Nano Lett.* **12** 5287–91
- [9] Senthilarasu S, Peiris T A N, García-Cañadas J and Wijayantha K G U 2012 Preparation of nanocrystalline TiO₂ electrodes for flexible dye-sensitized solar cells: influence of mechanical compression *J. Phys. Chem. C* **116** 19053–61

- [10] Bhuvana T and Kulkarni G U 2008 Polystyrene as a zwitter resist in electron beam lithography based electroless patterning of gold *Bull. Mater. Sci.* **31** 201–6
- [11] Shi E *et al* 2013 Colloidal antireflection coating improves graphene–silicon solar cells *Nano Lett.* **13** 1776–81
- [12] Han W, Li B and Lin Z 2013 Drying-mediated assembly of colloidal nanoparticles into large-scale microchannels *ACS Nano* **7** 6079–85
- [13] Wu Z *et al* 2004 Transparent, conductive carbon nanotube films *Science* **305** 1273–6
- [14] Doherty E M, De S, Lyons P E, Shmeliov A, Nirmalraj P N, Scardaci V, Joimel J, Blau W J, Boland J J and Coleman J N 2009 The spatial uniformity and electromechanical stability of transparent, conductive films of single walled nanotubes *Carbon* **47** 2466–73
- [15] Geng H Z, Kim K K, So K P, Lee Y S, Chang Y and Lee Y H 2007 Effect of acid treatment on carbon nanotube-based flexible transparent conducting films *J. Am. Chem. Soc.* **129** 7758–9
- [16] Tokuno T, Nogi M, Karakawa M, Jiu J, Nge T, Aso Y and Suganuma K 2011 Fabrication of silver nanowire transparent electrodes at room temperature *Nano Res.* **4** 1215–22
- [17] Lee J Y, Connor S T, Cui Y and Peumans P 2008 Solution-processed metal nanowire mesh transparent electrodes *Nano Lett.* **8** 689–92
- [18] Madaria A, Kumar A, Ishikawa F and Zhou C 2010 Uniform, highly conductive, and patterned transparent films of a percolating silver nanowire network on rigid and flexible substrates using a dry transfer technique *Nano Res.* **3** 564–73
- [19] De S, Higgins T M, Lyons P E, Doherty E M, Nirmalraj P N, Blau W J, Boland J J and Coleman J N 2009 Silver nanowire networks as flexible, transparent, conducting films: extremely high dc to optical conductivity ratios *ACS Nano* **3** 1767–74
- [20] Iglesias A S, Murias B R, Grzelczak M, Juste J P, Marzán L M L, Rivadulla F and Correa-Duarte M A 2012 Highly transparent and conductive films of densely aligned ultrathin Au nanowire monolayers *Nano Lett.* **12** 6066–70
- [21] Jung I, Dikin D A, Piner R D and Ruoff R S 2008 Tunable electrical conductivity of individual graphene oxide sheets reduced at ‘low’ temperatures *Nano Lett.* **8** 4283–7
- [22] Arco L G D, Zhang Y, Schlenker C W, Ryu K, Thompson M E and Zhou C 2010 Continuous, highly flexible, and transparent graphene films by chemical vapor deposition for organic photovoltaics *ACS Nano* **4** 2865–73
- [23] Jo G *et al* 2010 Large-scale patterned multi-layer graphene films as transparent conducting electrodes for GaN light-emitting diodes *Nanotechnology* **21** 175201–6
- [24] Gilje S, Han S, Wang M, Wang K L and Kaner R B 2007 A chemical route to graphene for device applications *Nano Lett.* **7** 3394–8
- [25] Wu J, Agrawa M, Becerril H A, Bao Z, Liu Z, Chen Y and Peumans P 2010 Organic light-emitting diodes on solution-processed graphene transparent electrodes *ACS Nano* **4** 43–8
- [26] Bae S *et al* 2010 Roll-to-roll production of 30-inch graphene films for transparent electrodes *Nat. Nanotech.* **5** 574–8
- [27] Kim K S, Zhao Y, Jang H, Lee S Y, Kim J M, Kim K S, Ahn J H, Kim P, Choi J Y and Hong B H 2009 Large-scale pattern growth of graphene films for stretchable transparent electrodes *Nature* **457** 706–10
- [28] Tolcin A C 2012 *Indium: US Geological survey mineral commodity summaries* **2012** 74–75
- [29] Kumar A and Zhou C 2010 The race to replace tin doped indium oxide: which material will win? *ACS Nano* **4** 11–14
- [30] Ginley D S, Hosono H and Paine D C 2011 *Handbook of Transparent Conductors* (Berlin: Springer)
- [31] Chopra K L, Major S and Pandya D K 1983 Transparent conductors—a status review *Thin Solid Films* **102** 1–46
- [32] Tao C S, Jiang J and Tao M 2011 Natural resource limitations to terawatt scale solar cells *Sol. Energy Mater. Sol.* **95** 3176–80
- [33] Gupta R and Kulkarni G U 2013 Holistic method for evaluating large area transparent conducting electrodes *ACS Appl. Mater. Interfaces* **5** 730–6

- [34] Wu H *et al* 2013 A transparent electrode based on a metal nanotrough network *Nat. Nanotechnol.* **8** 421–5
- [35] Guo H *et al* 2013 Copper nanowires as fully transparent conductive electrodes *Sci. Rep.* **3** 2323
- [36] Lu Y, Huang J Y, Wang C, Sun S and Lou J 2010 Cold welding of ultrathin gold nanowires *Nat. Nanotechnol.* **5** 218–24
- [37] Garnett E C, Cai W, Cha J J, Mahmood F, Connor S T, Christoforo M G, Cui Y, McGehee M D and Brongersma M L 2012 Self-limited plasmonic welding of silver nanowire junctions *Nat. Mater.* **11** 241–9
- [38] Zhu S, Gao Y, Hu B, Li J, Su J, Fan Z and Zhou J 2013 Transferable self-welding silver nanowire network as high performance transparent flexible electrode *Nanotechnology* **24** 335202–8
- [39] Tenent R C, Barnes T M, Bergeson J D, Ferguson A J, To B, Gedvilas L M, Heben M J and Blackburn J L 2009 Ultrasooth, large-area, high-uniformity, conductive transparent single walled carbon nanotube films for photovoltaics produced by ultrasonic spraying *Adv. Mater.* **21** 3210–6
- [40] Hu L, Kim H S, Lee J Y, Peumans P and Cui Y 2010 Scalable coating and properties of transparent, flexible, silver nanowire electrodes *ACS Nano* **4** 2955–63
- [41] Hellstrom S L, Lee H W and Bao Z 2009 Polymer-assisted direct deposition of uniform carbon nanotube bundle networks for high performance transparent electrodes *ACS Nano* **3** 1423–30
- [42] Gaynor W, Burkhard G F, McGehee M D and Peumans P 2011 Smooth nanowire/polymer composite transparent electrodes *Adv. Mater.* **23** 2905–10
- [43] Chung C H, Song T B, Bob B, Zhu R and Yang Y 2012 Solution-processed flexible transparent conductors composed of silver nanowire networks embedded in indium tin oxide nanoparticle matrices *Nano Res.* **5** 805–14
- [44] Sahin C, Selen A E and Emrah U H 2013 Optimization of silver nanowire networks for polymer light emitting diode electrodes *Nanotechnology* **24** 125202–9
- [45] Xu P, Mujumdar A S and Yu B 2009 Drying-induced cracks in thin film fabricated from colloidal dispersions *Drying Technol.* **27** 636–52
- [46] Yow H Y, Goikoetxea M, Goehring L and Routh A F 2010 Effect of film thickness and particle size on cracking stresses in drying latex films *J. Colloid Interface Sci.* **352** 542–8
- [47] Shi E *et al* 2012 TiO₂-coated carbon nanotube-silicon solar cells with efficiency of 15% *Sci. Rep.* **2** 884